Test Regime for Brushless DC Motor

Robotics Research Group, University of Texas at Austin
2002 Deliverable for
Thread 8 – Test Regime for Intelligent Actuators
November 1, 2002

PRINCIPAL INVESTIGATOR:
Dr. Delbert Tesar

PROGRAM MANAGER:
Dr. Mitch Pryor

RESEARCH ASSOCIATES:
Jae Gu Yoo

1. Introduction

There are no generalized data on the motor performance maps in the literature. The only data available are the separate results for different motors obtained from test beds run under constant loading conditions. Accordingly, one of the goals of this effort is to generalize the data in a form of generalized motor performance maps which could cover the whole family of the specific motor of different rated power under dynamic load operation.

In practice, motors operate in the factories with a changing environment such as different room temperatures, load and velocity profiles, and the type of tasks. As a result, the motor loading happens to be non-stationary and stochastic variables. However, the influence of load variation on motor performance has not received proper attention from engineers. That is, the motor catalogs and brochures are not presenting enough information about the response to non-linear, periodic loadings [1]. Therefore, the first goal of this study will be development of the test protocols to generate the motor performance maps under variable loadings. Additionally, the parasitic motor characteristic like torque ripple will be identified in different operating ranges. Finally, in order to cover completely the operational range of the specific motor, the test regime for the response time will be presented. All of the test regimes established in this report are based on the performance criteria developed in [10].

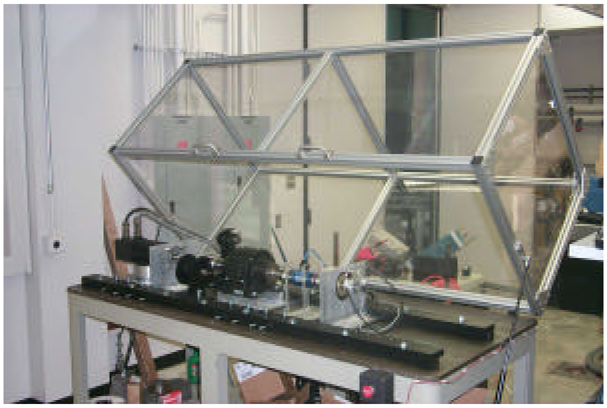

Figure 1. Nonlinear Test Bed

2. Measurement of the motor parameters

The Nonlinear Test Bed for Actuators shown in Figure 1 will incorporate a large number of variables to be used during the tests [11]. Variables will be determined at various locations in the system. Some of the parameters that will be useful to read out from the test bed are position, velocity, torque, temperature, voltage, current, and magnetic flux density. This set of data can be combined to represent specific performance criteria for the actuator. Depending on performance envelope, we can evaluate the output performance of the actuator in the specific range of criteria. Most of the parameters demand to select highly qualified sensors. Table 1 lists several dominant parameters and required sensors to test an actuator. An encoder or a potentiometer can measure position. In industry, people use encoders because it is possible to have more precise resolution. Velocity and acceleration can be obtained from the differentiation of position in the sensor. Also, the resolution of more than 22 bits is the critical value of selection in torque sensor because an even small amount of torque changes are recorded during the test. Magnetic flux density is also important to evaluate the performance of a motor because the maximum value of this quantity is the criteria to evaluate torque saturation. Usually, the Hall effect sensor is used to measure the magnetic signature [2]. In addition, thermocouples are used to measure the temperature inside the test motor but the difficult problem is how to implement the temperature sensor inside of the motor. A microphone might also be useful to measure the acoustic sound from the motor during operation.

Test Parameters	Sensor selection
position, velocity	Encoder
torque	Torque sensor
Current, voltage	Current sensor
Temperature	Thermister
Magnetic flux density	Hall effect sensor

Table 1.

3. Criteria Development

Before the test methods for Brushless DC Motor (BLDCM) are further discussed, the origin of the performance criteria should be mentioned in this section. From discussions with prime mover suppliers (motor catalogs), it is apparent that only general performance descriptions are provided. Examples of these are motor power, torque-speed relationship, motor efficiency, etc. Most of these parameters are one-dimensional and rarely two-dimensional.

In reality, a prime mover has a multitude of parameters that affect overall performance. A detailed understanding of these cross-couplings and parameters is an essential first step towards improved performance. Development of these criteria and the relationships among them is the foundation to this problem. An initial listing of l0 actuator performance criteria is given in Table 2. For example, the torque generated by a motor is closely tied to its temperature. Understanding of this relationship allows us to better address the cooling needs of the actuator for various duty cycles. Also, of interest is the acceleration response of a motor under a given load. Analysis of this property can provide us with an operational acceleration margin that can tell us how fast the acceleration follows the input torque command (i.e., in terms of step input). The difference between real output power and theoretical power computed via an analytical model is important for CBM. Such information can also allow us to anticipate power drop at higher temperatures. Sudden impacts can often result in actuator failure. As such, the torque/force impulse response of an actuator could be an essential decision making tool for an operator. Superimposed variations in the normal load (called torque ripple) affect actuator performance. This torque ripple has a distinct sound signature that can be detrimental for low noise applications such as deployment on submarines. At low speeds, a robot arm follows the desired path with some offset that causes tracking error. Friction in the bearings inside the actuator contributes to this offset. A detailed description of the proposed actuator criteria is presented in [10]. In this report, 6 out of 10 operational criteria for a prime mover are considered and 6 test regimes for them are suggested to obtain experimental data.

Criteria	Descriptions
Operational Margin	Indicates the maximum speed and torque with dynamic loads.
Temperature	Temperature may cause magnetic field degradation.
Efficiency	Output power divided by input power.
Motor Losses	How much copper and core losses are generated.
Response Time	How fast the response follows the input signal.
Acceleration	Limit of acceleration at various levels of torque.
Torque Impulse	Shock level relative to a given duty cycle norm.
Torque Saturation Limit	Torque saturation based on duty cycle norm.
Torque Ripple	Percentage of more uniform variation in the output torque.
Friction Torque	Can cause tracking error at lower speeds

Table 2. Initial Sets of Actuator Criteria

4. Test Regime for BLDCM

4.1 Torque-speed curve with dynamic loadings.

Generally, the torque-speed curve is obtained by increasing torque with a fixed value of speed in current mode. However, this torque-speed plot does not show whether it takes the deteriorated effect in several different kinds of loads such as sinusoidal, ramp, arbitrary nonlinear periodic loads. Given one of these loading types, several tests will be performed with different magnitudes and frequencies. The whole loading period will be at least one minute for each test in order to see the trajectory with different torque profiles. The generated torque will be recorded as a state at each time to compare the value of the measured state with the monitored state values obtained from a Condition Based Maintenance system in real time. In all of the tests with different dynamic loadings, it should be noticed that both amplifier and motion controller influence the performance of the test motor.

The example of the test procedure for the first criterion is represented in Figure 2. The amplifiers for the test motor and the load motor use current feedback. The motion of the load motor hinders and disturbs the motion of the test motor. Thus, the side effect generated between these two torque-generators cause the output shaft torque. Increasing or decreasing speed in the test motor can change the output torque measured from the torque sensor. Also, varying the magnitude and frequency of the load torque in the load motor can affect to the output torque obtained between these two motors. The test motor and the load motor cannot run independently at the start of the running. Because they are connected by a clutch on operation, the position and velocity feedbacks have to be assigned in the test motor only. The load motor will have only a torque feedback control loop. The test motor will start to run at the highest speed that the test motor can generate. The torque-speed curve will be obtained by reducing the speed, and in each speed region, the electrical torque command from the load motor will be increased until it arrives the highest value of the torque without changing the speed. The nonlinear periodic loading will be developed by four bar linkages, and the sinusoidal and ramp loadings will be performed by programmed torque from the load motor. In order to measure the loading torque, the test bed has a torque sensor which can measure up to 40 Nm. Each test will be repeated at least 20 times to allow for statistical analysis. The data obtained from all of the tests will be analyzed by generating the mean and standard error values with the proper assumption of normal distribution. As an initial set of torque-speed curve with respect to several different types of loadings, at least 20 performance maps for this criterion will be obtained. Ten maps are considered with 10 different levels of torque magnitudes in sinusoidal input loadings. Also, 10 additional maps will be obtained from arbitrary generated nonlinear periodic torque loadings in the load motor.

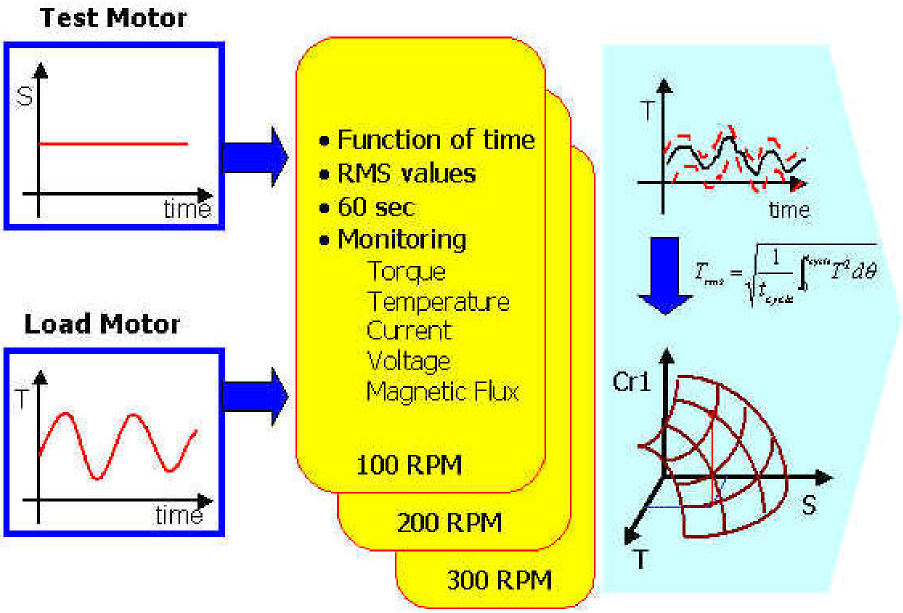

Figure 2. Torque speed curve with dynamic loading

4.2 Efficiency with respect to different types of torque and speed.

The operating efficiency is the most commonly used to evaluate motors and the different motor loads help to identify energy efficiency gains and possible reliability improvements. There were many methods to evaluate motors in the literature [1] and they tried to improve the accuracy of the efficiency evaluation for a targeted group of motors. To calculate exact and realistic value of efficiency, the following equation will be used in this testing.

$$Efficiency = \frac{Shaft\ output\ power}{Electrical\ input\ power} \tag{1}$$

The shaft output power is the input power minus the losses. How to assess losses is another test regime that we are going to discuss in the future. However, the shaft output can be measured at the torque sensor which is located between the load motor and the test motor in the test bed. Also, the electrical input power will be obtained from required current and voltage values generated in the test motor.

The test set up to obtain the performance maps for motor efficiency is elementary. The mechanical torque output signal is measured from the torque sensor and the speed of the test motor will be monitored at the same time. Also, the current and voltage in three phases are measured and recorded in real time. The detailed circuit design for current sensor and voltage divider is shown in [11]. The dynamic loadings generated from the load motor describe several different kinds of torque profiles. The first dynamic load is the sinusoidal wave. By changing the frequency and the amplitude in each load profile, the induced current will influence the output power. Also, another dynamic loading type will be the sharp edged nonlinear torque profile, which has peak torque periodically. By connecting this load profile to the test motor, how often regularly generated peak torque affects the motor efficiency will be known. There can be additional efficiency maps depending on how the torque is characterized from the load motor.

4.3 Temperature effect on torque-speed curve

In all of the electrical machines, the electrical, magnetic and thermal processes are internally coupled together in some sense. The temperature distribution is affected by the properties of the conducting and magnetic materials and the performance of the electromagnetic force, which is generated from the reaction between stator and rotor. The most temperature sensitive parameters are the stator winding resistance and the iron core of the stator [3]. Over the operational temperature range of the motor, the resistance variation with the temperature will be obtained. Figure 3 shows the test motor stator and four spots are chosen for the measurements of the temperature inside the motor. There are four holes through the front cover face of the stator and four thermisters are attached on the stator windings and core by using

Figure 3. Stator of PMSM

epoxy. The temperature sensors are attached to the stator as shown in Figure 4. The winding wires have insulation so actually the sensors measure the temperature on the insulation of the wires. However, it is too hard to find the way to measure the actual temperature of the wires, so in this test, when the temperature calculation is performed, the small additional weighting factor might be multiplied to the real measurement values with proper assumptions. This will need further research in the future. As mentioned in Section 4.1, the same torque profiles are generated in the load motor while the test motor runs at a certain speed to produce the torque-speed curve. At this time, there is one more measurement parameter, which is temperature. The operating temperature of the test motor is considered between $25\,°C$ (an ambient temperature) and $100\,°C$. The temperature values measured in four different spots inside the test motor will be recorded with respect to given torque and speed values to generate 3D plots. The experimental results including the variation of the temperature will provide the complete set of the electromechanical performance maps. Therefore, the first three criteria will be obtained at the same test setting and time.

4.4 Acceleration

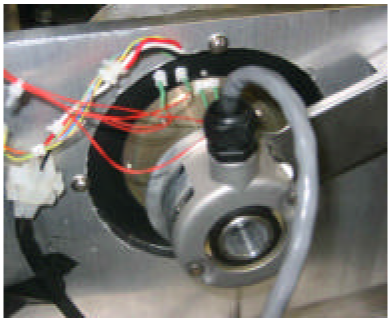

Figure 4. Stator with thermisters

Determining torque and speed capacity curve to cover the majority of the potential operating situations is not easy and time consuming. IEEE Standard 115 [4] lists several methods that can be employed to measure torque and current. One of the methods for measuring them is the acceleration test. Measurements taken by this method generate values for stator current, applied voltage, input powers, and input torque. By measuring the position from the encoder, the acceleration will be derived at the instant time of the differential changes in rotor speed. The acceleration tests are conducted at different values of loading torque and speed to build a valuable and meaningful motor performance map. A high acceleration capability requires a high maximum torque combined with a constant polar moment of inertia, J_m of the motor and is expressed as follows.

$$a = \frac{d^2q}{dt^2} = \frac{1}{J}\left(T_e - F_b\frac{dq}{dt} - T_m\right) \tag{2}$$

where a is the acceleration, q is the angular position, T_e is the electrically generated torque, F_b is the friction coefficient, and T_m is the load torque.

The major problem with the acceleration test is obtaining sufficient data points as motor speed approaches synchronous speed to be able to define the actual shape of the curve in a certain period of the testing. The optimum speed that produces a larger incremental acceleration in each time step should be found from this test by changing the level and frequency of the loading torques [5]. Another factor that affects the outcome of the acceleration test is the value used for the inertia. The moment of the inertia of the machines can be determined accurately from the results of the friction test for the mechanical frictions of motors, break, clutch and couplings.

Finally, the acceleration capability of a permanent magnet motor is limited by the demagnetization of the magnets. It can result from high temperature of the magnets and the winding insulation. The temperature increases the resistance of the winding wires and the increased resistance affects on the applied current to the motor. For example, at a temperature around $100^\circ C$, acceleration might be deteriorated as the torque generated by a reduced magnetic flux due to higher temperature.

4.5 Response time

As one example of the transient response tests, the response time will be measured at several torque and speed levels. The input source will be a step input to clearly identify the changes of the input. Figure 5 shows the torque response for a step change of the reference torque from –2 to 2 Nm when the rotor is blocked. It is seen that the torque response is as fast as predicted earlier and there is no overshoot. Also, there is the torque ripple with signal noise. From this figure, the response time can clearly be identified as 3.2 ms. This criterion test will generate performance maps for a number of torque and speed values. During the test, there must be a limit torque that never reaches to the desired value.

The response time is limited by the mechanical inertia and the performance of the motion controller. These values are fixed at first and never changed, so the inertia should be carefully calculated to obtain an exact value and it is recommended to install the best performance of the motion controller. This test will be repeated with both increased and decreased cases in several times. The speed response time will be obtained from no load test. Also, The torque response time data will be generated from the test set-up with locked rotor using the brake.

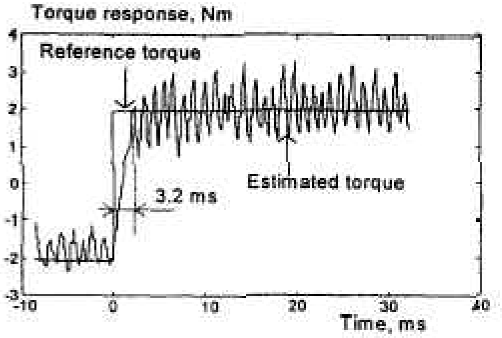

Figure 5. Step response of torque at standstill [6]

4.6 Torque ripple

A Permanent Magnet Synchronous Motor (PMSM), which is the test motor, generates parasitic torque pulsations owing to variable magnetic reluctance, distortion of the stator flux linkage distribution, and deficiencies of feasible winding geometries. The torque ripple is particularly undesirable in some demanding motion control and it leads to speed oscillations which cause deterioration in the performance [7]. Continuous constant torque from the test motor generates in order to identify the ripple on the output torque curve. The torque ripple will be measured in the following equation.

$$T_r = \frac{Peak-to-Peak\ Torque\ Ripple}{AverageOutput\ Torque} \times 100\ (\%) \qquad (3)$$

If the load motor is used to generate the constant torque, the measurement data from the torque sensor cannot be identified which motor out of the test motor and the load motor develops more torque ripple. Therefore, the constant torque will be applied from the brake loading. The static brake generates a lot of heat so it is applied a very short time (i.e. one or two seconds). Also, the output signal from the torque sensor should be filtered using an active filter to eliminate measurement noise.

5. Performance Envelopes

Once all the performance maps based on the suggested operational criteria are obtained for several different kinds of phenomena, the performance envelopes have to be generated based on them. Even though the torque-speed curve with respect to temperature and the efficiency at a given speed and torque are specified in the trade literature (or arrived at through simulation), the actual values will depend on the type of output load. Therefore, if the performance envelope including all of these cases is completed, it will become the criteria map to guide the operation of the motor. Figure 6 schematically suggests how each performance envelope is obtained from several actuator criteria. The Robotics Research Group (RRG) at the University of Texas at Austin has developed the Nonlinear Test Bed for Actuators in order to obtain enough information to evaluate the performance of a specific motor. The test bed might make it possible to interpret more actuator criteria with further study. The data obtained from the sensors in the test bed are plotted with respect to time. The data sets obtained from the repetition of testing a motor are ready to insert in the multivariate statistical analysis. The mean value with high confident intervals (95%) should be calculated and then several different plots of mean values in different loading conditions are drawn. Along with the curves, upper and lower boundaries are also decided from the statistical calculation. Once all of the data sets are collected from the sensors, they are combined together based on each actuator criterion. Then, performance maps can be completed if these actuator criteria put together based on appropriate independent parameters. From the performance maps built in

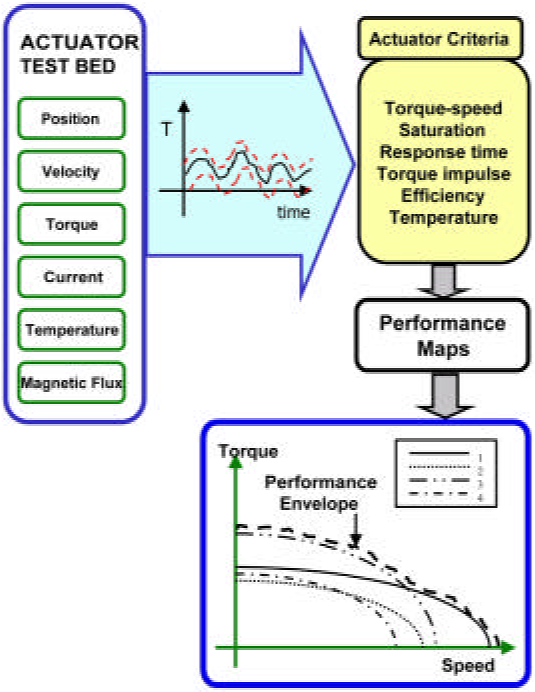

Figure 6. Performance envelope development

the suggested test methods, we have to find out which of the independent parameters will be used as the controllable axis in the performance envelope graphs. These graphs need to demonstrate the actual performance in the reference motor. There is an example about how the performance envelope is generated with respect to torque and speed at the bottom of Figure 6. It is assumed that line 2 (a dotted line) is drawn as torque is obtained at each constant speed with the condition of 80% of efficiency. If the motor accepts 50% of efficiency, then the torque speed curve line might be increased with a small amount. This is line 1 (a solid line). Additionally, let's assume two more lines are drawn with respect to temperature. Given the same time duration, a constant torque is applied to the test motor at a given constant speed and a temperature sensor measures the temperature of the stator winding temperature. The line 4 (the combined lines of a dot and a solid) assumes the stator temperature keeps 60 $°C$ at a given torque and speed, respectively. If it is allowed up to 80$°C$, the torque-speed curve might be increased as shown in line 3 (the combined lines of two dots and a solid). All of these four lines, which come from two actuator criteria, are plotted along two independent parameters (torque and speed). The performance envelope is determined with 30% of performance reduction as shown in Figure 6.

In summary, actuator performance maps must be obtained by simulation and experiment based on several independent control parameters. These independent parameters for PMSM drives are desired torque, rotor speed and current (or voltage). The voltage is needed to induce current, so one of them is used as the independent parameter. Also, the measured dependent parameters are output torque, temperature, magnetic flux density, acceleration, and response time. The independent parameters will be one of the x-y axes in Figure 6. Also, the combination of dependent parameters will be plotted in the third axis. In addition, the parameters estimated from the embedded sensors in the test bed will include signal noise, so some mathematical tools are considered to reduce this noise. One possible tool is the Kalman filter but it needs further study. The control parameters obtained through one of the signal filters should be confirmed by seeing how actuators operate in the actual system.

6. Conclusion and Future Work

This report presents a work-in-progress that aims to develop the performance criteria test regimes for the nonlinear testing of an actuator. An actuator is a highly non-linear device with redundant resources and that its performance can be improved by using a non-linear model and extensive sensory information. A collection of performance maps is our approach of representing the complexity of the actuator (both model and sensor) as well as metrics for measuring the actuator state. These maps obtained from actuator criteria can be used to build performance envelopes, and to provide an operational capability for CBM and fault-tolerance. For performance envelopes, the parameters in each criterion are carefully investigated as to whether they are controllable and independent. Then, these are manipulated as common factors to get the unique performance envelope for the actuator. The test data developed from each test regime must be normalized and made homogeneous:

for instance, it may be necessary that all criteria be described for values between 0 and 1, with 1 being the desirable value. Great difficulty appears when the bounds for the map are unknown. The 6 different test regimes developed in this report apply only to the prime mover and specifically to BLDCM. Further work involves developing more test regimes to generate performance maps that represent complete actuator behavior.

7. References

[1] John Hsu, John Kueck, Mitchell Olszewski, Don Casada, Pedro Otaduy, and Leon Tolbert, "Comparison of Induction Motor Field Efficiency Evaluation Methods," *IEEE Transactions on Industry Applications*, Vol.34, No.1, January 1998

[2] *DC Motors, Speed Controls, Servo Systems*, The electro-craft engineering handbook, Rockwell Automation/Electro-Craft, 5th Ed.

[3] G. R. Slemon and A. Straughen, "*Electric Machines*," 1980, Reading, Massachusetts: Addison-Wesley Publishing Company.

[4] Test Procedures for Synchronous Machines, "*Part I – Acceptance and Performance Testing; Part II – Test Procedures and Parameter Determination for Dynamic Analysis*," IEEE 115-1995.

[5] K.L. Shi, Y.K. Wong, and S.L. Ho, "A Rule-Based Acceleration Control Scheme for an Induction Motor," *IEEE Transaction on Energy Conversion*, Vol.17, No.2, June 2002

[6] M.F. Rahman and L. Zhong, "Comparison of Torque Responses of the Interior Permanent Magnet Motor Under PWM Current and Direct Torque Controls," *IECON Proceedings of Industrial Electronics Society, The 25th Annual Conference of the IEEE* , Vol.3 , 1999, pp. 1464 – 1470

[7] Joachim Holtz and Lothar Springob, "Identification and Compensation of Torque Ripple in High-Precision Permanent Magnet Motor Drives," *IEEE Transaction on Industrial Electronics*, Vol.43, No.2, 1996, pp.309 - 320

[8] J. R. Hendershot and T.J.E. Miller, "*Design of Brushless Permanent-Magnet Motors*," 1994, Magna Physics Publishing and Clarendon Press, Oxford Science Publications.

[9] Agustin Vasquez, "Condition-Based Maintenance of Actuator Systems Using a Model-Based Approach," Dissertation in the University of Texas at Austin, 2000.

[10] Jae Gu Yoo, "Performance Criteria Development for Switched Reluctance Motor," Technical report, 2002 Deliverable for Thread 6 ONR-All Electric Ship (AES) program, December 2002

[11] Jae Gu Yoo, Paul Hvass, and Julie Linsey, "Test Bed to Measure the Performance Criteria of Actuators," Technical report, 2002 Deliverable for Thread 3 ONR-All Electric Ship (AES) program, December 2002